

# INSAR RADARGRAMMETRY : A SOLUTION TO THE PHASE INTEGER AMBIGUITY PROBLEM FOR SINGLE INTERFEROGRAMS

Andrew Sowter<sup>(1)</sup>, John Bennett<sup>(2)</sup>

<sup>(1)</sup>*IESSG, University of Nottingham, University Park, Nottingham NG7 2RD, UK  
Email: andrew.sowter@nottingham.ac.uk*

<sup>(2)</sup>*SCEOS/EEE, University of Sheffield, Mappin Street, Sheffield, S1 3JD, UK  
Email: J.C.Bennett@sheffield.ac.uk*

## ABSTRACT

The interferometric phase in a SAR interferogram may only be represented in the range 0-360 degrees, leaving an unknown integer ambiguity representing the number of extra whole wavelengths travelled during the imaging at the second antenna. This makes it impossible to solve for the precise baseline components from the interferogram alone. In this paper, the InSAR geometry is re-examined using a radargrammetric approach that proposes the use of space triangulation to determine target position and height. From this approach, a solution to the phase integer ambiguity is proposed that requires only coarse, sparse ground control to enable the 3D location of all points within an interferogram to be determined. Furthermore, the solution implies that precise differential InSAR may be applied over all terrain types without the use of an accurate DTM. This solution allows further automation of the technique, enables fast responses to events in remote, unmapped areas and negates the requirement to build up a vast map archive to support a global InSAR mission. The results are illustrated using experimental data from the GB-SAR facility at the University of Sheffield.

## 1 INTRODUCTION

SAR interferometry is, and continues to be, a technique of great interest in geophysical remote sensing. Over the last 10-15 years, InSAR has proved itself to be a major tool in the monitoring of land deformation at centimetric accuracies [1], earthquakes [2], volcanoes [3], ice sheets [4], landslides [5] and terrain subsidence [6].

In essence, the interferometric technique has many similarities with GNSS where precise motion requires the analysis of carrier phase. In InSAR, the receiver is also the transmitter, meaning that the phase is related to the two-way delay, complicated further by the scattering mechanism of the target. If the scattering mechanism is unchanged from a different receiver position, the signals are correlated and the difference in carrier phase between the two positions can be calculated.

Like GNSS, the resulting phase difference can only be determined modulo  $2\pi$  leaving a problem in that an integer phase ambiguity remains. In GNSS, there have been several methods proposed for its solution [7-9] and some of these have been directly applied to the InSAR problem [10] albeit using many, stacked, interferograms.

Sowter [11] has proposed a method for the determination of the phase ambiguity for single SAR interferograms that has clear repercussions for the use of InSAR for monitoring land movements. This paper contains a re-development of the differential InSAR concept assuming the phase ambiguity is known and demonstration of its application in a controlled, laboratory environment.

## 2 INSAR GEOMETRY

The analysis contained in this part of the paper follows the conventions of [11] throughout.

Consider the imaging geometry of a two-pass InSAR system where the two antennas are at points  $P_1$  and  $P_2$  and are both imaging a target at  $T$  (Fig. 1).

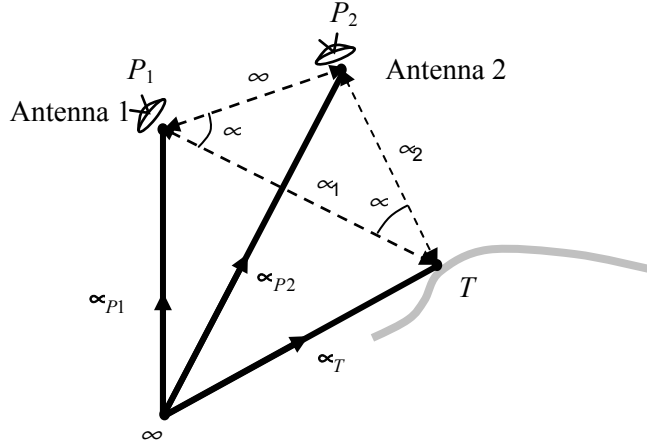


Fig. 1. Typical InSAR Geometry

The full 3-d location of the target at  $T$  may be found by solving the three equations:

$$f_{D1} = -\frac{2}{\lambda |\rho_T - \rho_{P1}|} (\rho_T - \rho_{P1}) \lambda \mathbf{v}_{P1}$$

$$\rho_1 = |\rho_T - \rho_{P1}|$$

$$\frac{\rho_1}{\lambda} + \frac{\rho_2}{\lambda} \mathcal{N}^{12} + \rho_e = \frac{|\rho_T - \rho_{P1}|^2 - |\rho_T - \rho_{P2}|^2 + B^2}{2|\rho_T - \rho_{P1}|}$$

where  $f_{D1}$  is the Doppler frequency,  $\lambda$  is the radar wavelength,  $\mathbf{v}_{P1}$  is the satellite velocity vector at  $P_1$ ,  $\rho$  is the interferometric phase, measured modulo  $2\pi$ ,  $\mathcal{N}^{12}$  is the interferometric integer phase ambiguity and  $\rho_e$  is the far field correction factor, given by:

$$\rho_e = \frac{B^2 - (\rho_1 - \rho_2)^2}{2\lambda \rho_1}$$

Numerically,  $\rho_e$  is very small compared to the Baseline and changes very little across an image. However, it is of the order of a wavelength and therefore cannot be ignored for precise applications that use the phase value. A good initial estimate for  $\rho_e$ , applicable across the whole image, may be found through substitution of the pseudo-range values into equation 4.

The main problems with the solution of the above lie the identification of the integer phase ambiguity,  $\mathcal{N}^{12}$ , the estimation of the range value,  $\rho_1$ , and the value of the orbital baseline,  $B$ . In [11] it is shown that  $\mathcal{N}^{12}$  can be identified unambiguously through the use of an ambiguity search process and relatively coarse ground control, assuming baseline refinement has been applied. Some 4000 ambiguity values may need to be assessed in the process, depending on the specific imaging geometry.

The condition on the ground control is that the estimated locational accuracy,  $\sigma_T$  of the target is such that:

$$\sigma_T < \frac{\rho_1 \lambda}{4B \sin \alpha}$$

This condition not only includes target error but also errors relating to the radar, such as range and baseline effects. For a typical ERS-type configuration, the right hand side of the equation will have a value of around 75m. It is interesting to note that this value is related to the ambiguity height [12] which is used to assess the application of a low-accuracy DSM in an InSAR processing chain.

To generate a digital surface model (DSM), the value of  $\phi^{12}$  is needed for all pixels across the whole interferogram, a not inconsiderable task if the ambiguity search process is applied everywhere. However, if  $\phi^{12}$  is determined for a single point and the phase is unwrapped from this solved point, any change in  $\phi^{12}$  would be compensated by the unwrapped value of  $\phi$ . For areas isolated from a simple unwrapping procedure, such as those bounded by an impassable low coherent area, such as open water or dense forest, another control point needs to be found within the isolated area to form a start point for a second unwrapping process. Thus, the rigorous geolocation algorithm need not be applied across the whole image.

The range value  $r$  cannot be simply related to the transmit-receive time (pseudo-range) as this will certainly be affected by tropospheric delay [13]. However, the value used is within 10m of the actual value, assuming ERS-type errors [14].

The orbital baseline has perhaps the most serious effect on the accuracy of InSAR [15] and some baseline refinement is certainly required to meet most acceptable standards of precision [16, 17].

For the following analysis it is assumed without loss of generality that the effects of errors has been minimised through baseline refinement, the selection of highly coherent targets and there being no change in atmospheric properties between acquisitions.

### 3 PHASE DEVIATION

In an error-free differential interferometry scenario, an entirely feasible methodology would be to calculate the full 3-d positions of the same target in two interferograms and to examine its displacement. However, this impossible in the real world, mainly due to the pseudo-range approximation, and therefore it is usual to examine the interferometric phase change between the interferograms and to infer target motion from that value alone [18].

The interferometric phase is related to the baseline declination angle by:

$$\frac{4\pi}{\lambda} \cos \theta = \frac{1}{B} \left( \phi + 2\pi \phi^{ij} + \frac{4\pi}{\lambda} \phi \right)$$

It can be shown [19] that the phase deviation between two interferograms,  $\Delta\phi$ , is defined by:

$$\Delta\phi = \frac{1}{B_{12}} \left( \phi_{12} + 2\pi \phi^{12} + \frac{4\pi}{\lambda} \phi_{12} \right) - \frac{1}{B_{13}} \left( \phi_{13} + 2\pi \phi^{13} + \frac{4\pi}{\lambda} \phi_{13} \right) - \frac{8\pi \sin \frac{1}{2} \theta}{\lambda} \sin \left( \phi_{12} + \frac{1}{2} \Delta\phi \right)$$

which is zero when there has been no differential change in target position.

An objective of differential InSAR is to calculate the phase deviation,  $\Delta\phi$ , for all pixels in the two interferograms. Any deviation from zero indicates an error or a change in one of the phase values, possibly indicating a change in target position at the third acquisition. If there has been a change in position, the range to the target  $T$  will be shorter or longer than anticipated and therefore the phase value will be different from the anticipated value.

This method outlined above is an extremely precise method for the derivation of the differential phase change. The assumptions are:

- ∞ The baseline is known very accurately;
- ∞ The phase must be unwrapped;
- ∞ Coarse ground control is available.

If all of these assumptions are satisfied, precise differential interferometry can be performed without recourse to using a DSM or using the far-field approximation.

#### 4 GB-SAR

GB-SAR is a ground-based microwave sensor system developed in the Department of Electronic & Electrical Engineering (EEE) from funding awarded to the Sheffield Centre for Earth Observation Science (SCEOS) by the Natural Environmental Research Council (NERC). The indoor facility is an anechoic facility which offers the user a precision, highly-controlled, repeatable measurement environment [20-22].

The facility is illustrated in Fig. 2 where a vegetation canopy is being imaged by the horn antennae, mounted on a rack in the ceiling. From the mounting, the antenna is able to image from a variety of positions in 2-d, the positions being known to an accuracy of less than 1mm. Through the processing of echoes gathered along a lateral path it is possible to fully simulate a SAR acquisition in terms of amplitude and phase.



Fig. 2. The GB-SAR Indoor Facility

The facility is able to image in L, S, C and X bands using the full range of polarisations over a range of incidence angles if required. Therefore, GB-SAR offers an idea environment for the testing interferometric measurements under strictly controlled conditions.

#### 5 THE EXPERIMENT

For the purposes of testing the ambiguity search algorithm, interferometric results from an earlier project were used (NERC CORSAR Programme, courtesy of Dr Paul Saich, UCL). In that project, fifteen trihedral reflectors were placed at known positions on a vertical board above a soil bed (Fig. 3). These were imaged from a variety of positions on the rack in the ceiling using a radar of a fixed 3cm wavelength.

As the Doppler Equation does not apply to SAR data acquired in this way, only measurements from the central three trihedrals were considered in the analysis as it was assumed that they had the same squint angle to the radar. Using this data, phase measurements of the trihedrals were taken from many different positions in the rack, enabling the construction of baselines ranging from 2cm to 32cm in length.

The objectives of the experiment were to reconstruct the positions of the three trihedrals using the ambiguity search method and to show that the line-of-sight target deviation was close to zero, as the targets did not move between measurements.



Fig. 3. The position of the trihedral reflectors in the GB-SAR facility

## 6 RESULTS

The positions of the targets were reconstructed for a variety of baselines using ambiguity searching. This was undertaken for the lower target only (the reference target), the position of the remaining targets being derived from the unwrapped phase, relative to the reference. A point on the soil surface was used to seed the search. The results are shown in Fig 4(a). In general, the target positions were derived in agreement with expectations, given the assumption that the targets had the same squint angle. The distribution of solutions for the uppermost target was wider than those lower. This was due to uncertainty in the far field correction parameter  $\omega$ . This parameter is estimated and is improved by iteration but may still cause errors when the baseline to range ratio is high. It would not be expected to find the same degree of error in the spaceborne case.

The results for the line-of-sight deviation are shown in Fig. 4(b). Again, the results are acceptable, with the higher target showing the greater value, again due to the estimation of  $\omega$ .

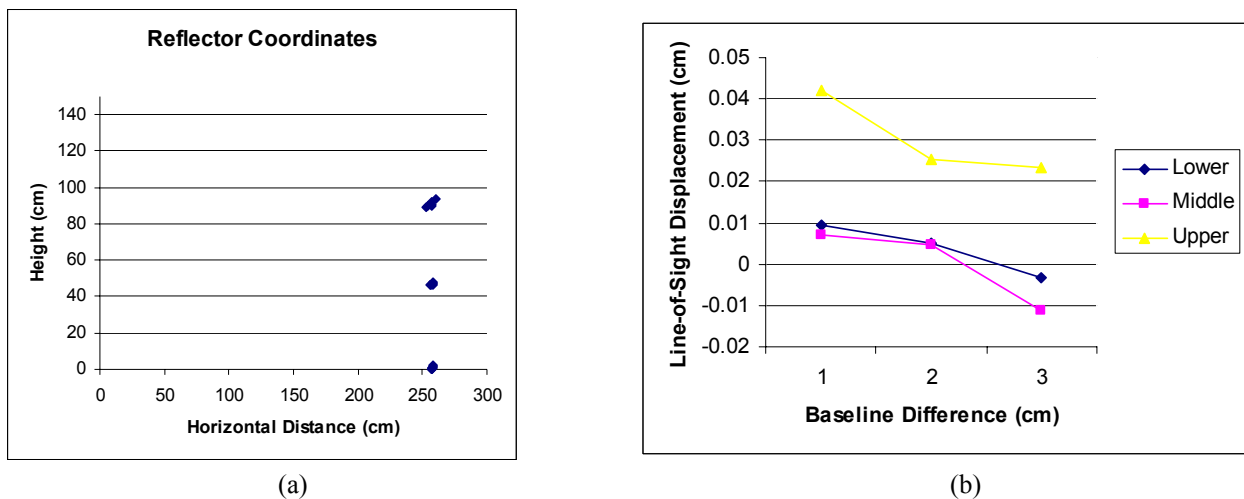


Fig. 4. The experimental results (a) for the target positions and (b) for the line-of-sight displacement.

## 7 CONCLUSIONS

The experimental results have clearly shown the validity of the ambiguity search method using coarse ground control. In this way, the phase ambiguity can be identified unambiguously and, using a radargrammetric solution of three geometric equations, the full 3-d position of a target can be found. Furthermore, it has been demonstrated that, if the

interferometric phase can be unwrapped, the position of all targets in an unwrapped region can be derived when the search process is applied to a single reference point only. Also, and perhaps more importantly, the phase deviation has been shown to be derived with a knowledge of the integer ambiguity only. This implies that land and ice motion may be mapped without explicit use or derivation of a DSM. As this is becoming an important application of InSAR, it may help in the application of DInSAR in remote areas where a DSM is not available or in the swift reaction to sudden, cataclysmic events where access to a DSM may be costly and time consuming.

The process described in this paper is the subject of Patent Application Number 0316858.0.

## 8 REFERENCES

1. Zebker, H.A., Werner C.L., Rosen P.A. and Hensley S., Accuracy of topographic maps derived from ERS-1 interferometric radar, *IEEE Transactions on Geoscience and Remote Sensing*, 32(4), 823-836, 1994.
2. Massonnet, D., Rossi, M., Carmona, C., Adragna, F., Peltzer, G., Feigl, K. and Rabaute, T., The displacement of the Landers earthquake mapped by radar interferometry, *Nature*, 364, 138-142, 1993.
3. Briole, P., Massonnet, D. and Delacourt, C., Post-eruptive deformation associated with the 1986-87 and 1989 lava flows of Etna detected by radar interferometry, *Geophysical Research Letters*, 24(1), 37-40, 1997.
4. Goldstein, R., Engelhardt, H., Kamb B. and Frolich, R., Satellite radar interferometry for monitoring ice sheet motion: Application to an Antarctic ice stream. *Science*, 262, 1525-1530, 1993.
5. Fruneau, B., Achache, J. and Delacourt, C., Observation and modelling of the Saint-Etienne de Tinee landslide using SAR interferometry. *Tectonophysics*, 265(3-4), 181-190, 1996.
6. Massonnet, D., Holtzer, T. and Vadon, H., Land subsidence caused by the East Mesa geothermal field, California, observed using SAR interferometry. *Geophysical Research Letters*, 24(8), 901-904, 1997.
7. Abidin, H.Z., On-the-fly ambiguity resolution. *GPS World*, 5(4), 40-50, 1994.
8. Leick, A., *GPS Satellite Surveying*, Second Edition, John Wiley & Sons, Inc., 1995.
9. Han, S. and Rizos, C., Comparing GPS ambiguity resolution techniques. *GPS World*, 8(10), 54-61, 1997.
10. Hanssen, R.F., Teunissen, P.J.G. and Joosten, P., Phase Ambiguity Resolution for Stacked Radar Interferometric Data, *Proceedings of the International Symposium on Kinematic Systems in Geodesy, Geomatics and Navigation*, Banff, Canada, 5-8 June, 317-320.
11. Sowter, A., Phase Ambiguity Determination for the Positioning of Interferometric SAR Data. *Photogrammetric Record*, 18(104), 308-324, 2003.
12. Massonnet, D. and Feigl, T., Radar interferometry: limits and potential. *IEEE Transactions on Geoscience and Remote Sensing*, 31(2), 455-464, 1993.
13. Tarayre, H. and Massonnet, D., Atmospheric propagation heterogeneities revealed by ERS-1 interferometry. *Geophysical Research Letters*, 23(9), 989-992, 1996.
14. Sowter, A., Smith, D.J., Laycock, J.E. and Raggam, H., An error budget for ERS-1 SAR imagery. *GEC-Marconi Research Centre Report under ESA Contract 7689/88/HE-I*, 1990
15. Li, F.K. and Goldstein, R.M., Studies of multibaseline spaceborne interferometric synthetic aperture radars. *IEEE Transactions on Geoscience and Remote Sensing*, 28(1), 88-97, 1990.
16. Zebker, H.A., Rosen, P.A., Goldstein, R.M., Gabriel, A. and Werner, C.L., On the derivation of coseismic displacement fields using differential radar interferometry: The Landers earthquake. *Journal of Geophysical Research*, 99(B10), 19617-19634, 1994.
17. Small, D. (1998). Generation of Digital Elevation Models through Spaceborne SAR Interferometry. *Remote Sensing Series, Volume 30, Department of Geography, University of Zurich, Zurich, Switzerland*, 1998.
18. Gabriel, A.K., Goldstein, R.M. and Zebker, H.A., Mapping Small Elevation Changes over Large Areas: Differential Radar Interferometry. *Journal of Geophysical Research*, 94(B7), 9183-9191, 1989.
19. Sowter, A., The derivation of phase integer ambiguity from single InSAR pairs: implications for differential interferometry, *Proceedings of the 11<sup>th</sup> FIG Symposium on Deformation Measurements, Santorini, Greece*, 149-156, 2003.
20. Morrison, K., Bennett, J.C., Cookmartin, G. and Quegan, S., "Development and capabilities of the Ground-Based SAR (GB-SAR) Facility". Proceedings of Advanced SAR Conference, Montreal, Canada, 25-27 June, 2003.
21. Morrison, K., Brown, S.C.M., Bennett, J.C., Cookmartin, G. and Quegan, S., "Ground-Based 3D polarimetric SAR tomography of vegetation canopies". Proceedings of Advanced SAR Conference, Montreal, Canada. 25-27 June, 2003.
22. Brown, S.C.M., Quegan, S., Morrison, K., Bennett, J.C. and Cookmartin, G., "High resolution measurements of scattering in wheat canopies – implications for crop parameter retrieval", *IEEE Transactions on Geoscience and Remote Sensing*, 41, 1602-1610, 2003.